CARBON 48 (2010) 1799–1806

available at www.sciencedirect.com

ScienceDirect

journal homepage: www.elsevier.com/locate/carbon

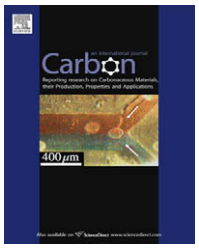

Study of fire retardant behavior of carbon nanotube membranes and carbon nanofiber paper in carbon fiber reinforced epoxy composites

*Qiang Wu, Wei Zhu, Chuck Zhang *, Zhiyong Liang, Ben Wang*

Department of Industrial and Manufacturing Engineering, High-Performance Materials Institute, FAMU-FSU College of Engineering, Florida State University, USA

ARTICLE INFO

Article history:
Received 8 November 2009
Accepted 14 January 2010
Available online 20 January 2010

ABSTRACT

Single-walled carbon nanotube (SWCNT) and multi-walled carbon nanotube (MWCNT) membranes (buckypaper) and carbon nanofiber (CNF) paper were incorporated onto the surface of epoxy carbon fiber composites, as proposed fire shields. Their flammability behaviors were investigated by a cone calorimeter. SWCNT buckypaper and CNF paper did not show notable improvement on fire retardancy. However, MWCNT buckypaper acted as an effective flame-retardant shield, reducing the peak heat release rate by more than 60% and reducing smoke generation by 50% during combustion. The pore structures of buckypapers and CNF paper were characterized by scanning electron microscopy (SEM), mercury intrusion porosimetry, and N_2 adsorption isotherms. Gas permeability of buckypaper and carbon nanofiber paper was measured. The correlation between buckypaper and CNF paper properties and their fire retardancy was discussed.

1. Introduction

Various applications of carbon nanotubes are expected to result from their unique structural, electrical, thermal, and mechanical properties [1–5]. Carbon nanotubes are being considered as a candidate flame retardant additive [6]. Using thermogravimetric analysis (TGA) and cone calorimeters, several groups have reported improved thermal stability and flame retardancy of nanotube/polymer composites. Kashiwagi et al. [6–9] found that carbon nanotubes act as flame-retardant fillers. They attribute the improved flame resistance to the formation of a protective nanotube network structure that acts as a heat shield for composites. Consistent with this mechanism, the flame retardancy was found to improve with better dispersion, higher loading, and a higher interface area (aspect ratio) of the nanotubes.

Buckypapers (carbon nanotube membranes) are free-standing mats of tangled carbon nanotube ropes [10], which can be fabricated by the filtration of carbon nanotube suspensions. Electrical conductivity [11], field emission properties [12], gas permeability [13–15], electronic and mechanical properties of buckypaper have been studied [16]. Many research efforts have been conducted to explore the potential applications of buckypaper, including carbon nanotube actuators [17], artificial muscles [18], strain sensors [19], electromagnetic interference (EMI) shielding [20], cold-field emission cathodes [12], and buckypaper epoxy composites [21]. Kashiwagi [7] found that the forming of a continuous structured network with no cracks would result in a protective barrier that would slow down mass loss rate and material flammability. The free standing buckypaper has a compact network structure due to the small diameter of carbon nanotubes. Dense nanotube networks and small pore size within the buckypaper provide low gas and mass permeability, which means buckypaper may act as an inherent flame-retardant shield when applied to the polymeric material surface.

* *Corresponding author:* Fax: +1 850 410 6342.
E-mail address: chzhang@eng.fsu.edu (C. Zhang).
0008-6223/$ - see front matter
doi:10.1016/j.carbon.2010.01.023

Recently, our research team dramatically improved flame retardancy of composites by placing SWCNT buckypapers onto the surface of polyhedral oligomeric silsesquioxane (POSS)/glass fiber composites [22]. Carbon nanofiber paper was also studied as a fire retardant sheet by another research group [23].

The main flame retardant function of buckypaper, or CNF paper, is that of preformed carbon nanotubes or nanofiber sheets acting as a protective layer which limit the transfer of decomposition gases from the polymeric matrix underneath. The combustible gases can be physically separated from the oxygen, preventing the combustion process from being sustained. In the present study, the flame retardancy of SWCNT and MWCNT buckypapers and carbon nanofiber (CNF) paper on the epoxy/carbon fiber composites' surface were compared by cone calorimetry tests. The pore structures of buckypaper and CNF paper were determined by scanning electron microscopy, N_2 physisorption, and mercury intrusion method. The gas permeability of air through buckypapers and CNF paper was also measured. The effect of the properties (pore structure, gas permeability) of buckypaper and CNF paper on the flame retardancy of composites was compared.

2. Experimental

2.1. Materials

HiPco SWCNTs purchased from Carbon Nanotechnologies, Inc., has a diameter of 0.8–1.2 nm and a length of 100–1000 nm. MWCNTs obtained from Thomas Swan, Inc., has a diameter of 20–30 nm and a length of 1–10 μm. The carbon nanofibers (PR-25-XT-PS) were kindly supplied from Applied Sciences, Inc., which has a diameter of 100–200 nm and a length of 50–100 μm. The epoxy matrix consisted of Epon 862 (diglycidyl ether of bisphenol F) with curing agent EPI-CURE W (diethylene toluene diamine) were both from Miller-Stephenson Chemical Company, Inc. IM 7 carbon fiber fabrics (style 4178, 5HS weave, 400 g/m^2, Textile Products, Inc.) were used as reinforcement.

2.2. Carbon nanotube membranes (buckypaper) and carbon nanofiber paper preparation

SWCNTs or MWCNTs were grinded in a mortar with a small amount of de-ionized water and Triton X-100 (from Alfa Aesar CAS number 9002-03-1). After grinding, the mixture was subsequently diluted and sonicated using a probe sonicator (Misonix sonicator® 3000, power 100 W, Frequency 20 kHz) for 1 h to make a stable suspension of carbon nanotubes. Each of the dispersions was prepared by sonicating 40 mg SWCNT or MWCNT powders in 1000 ml of 0.4 wt.% Triton X-100/de-ionized H_2O solution. Buckypapers were prepared by filtering a carbon nanotube suspension through a Nylon membrane on a home-made 9 in × 9 in funnel with the aid of a pressure pump [21]. Following filtration, the buckypapers were washed with water and isopropanol to remove the most of surfactant. Carbon nanofiber papers were prepared by filtering a carbon nanofiber suspension in isopropanol through a Nylon membrane on a home-made 9 in × 9 in funnel under vacuum. After air drying, the buckypapers or the CNF paper were peeled from the membranes. SWCNT, MWCNT buckypapers, and CNF paper were self-supporting mats, appearing as uniform, smooth, and crack-free paper-like sheets. Properties of the resulting SWCNT, MWCNT buckypapers, and CNF paper were summarized in Table 1.

Table 1 – Properties of the buckypapers and the CNF paper.

Sample	Size (cm × cm)	Thickness (μm)	Surface density (mg cm^{-2})
SWCNT buckypaper	21.6 × 21.6	15–20	1.29
MWCNT buckypaper	22.8 × 22.8	20–25	1.54
CNF paper	22.8 × 22.8	55–75	3.08

Table 2 – Compositions of different composite panels.

Sample	IM 7(g)	Epoxy (g)	Buckypaper or CNF paper (g)	Sample weight (g)
Epoxy/IM-7	24	12.6	0	36.6
Epoxy/IM-7/SWCNT-BP	24	13.0	0.4	37.4
Epoxy/IM-7/MWCNT-BP	24	12.7	0.5	37.2
Epoxy/IM-7/carbon nanofiber paper	24	13.4	0.6	38.0

2.3. Composite preparation

The Epoxy/IM-7 composites with and without buckypaper skins were fabricated by processing the composites using hand lay-up followed by vacuum bagging. The composites were cured at 121 °C for 2 h and at 177 °C for an additional 2 h, then cooled to ambient temperature. For control composites, six layers of IM 7 carbon fiber fabrics were incorporated in the composite laminates. For composites with buckypaper skin, one piece of buckypaper was placed at the top and two pieces of buckypaper placed at the bottom of carbon fiber laminates on a mold. The bottom sides of the composites, with two pieces of buckypaper, were facing up during cone calorimeter test, since a conical radiant electrical heater uniformly irradiates the sample from above. For composites with CNF paper, only one piece of CNF paper was placed at each side of composite. Compositions of different composites panels are listed in Table 2.

2.4. Testing

2.4.1. Characterization of the SWCNT, MWCNT buckypapers and carbon nanofiber paper

Scanning electron microscopy (SEM) was performed on a JEOL JSM-7401F field-emission scanning electron microscope. Micropore and mesopore size distributions and Brunauer–Emmett–Teller (BET) surface areas were determined using a Micromeritics Tristar system. Nitrogen adsorption isotherms were collected at 77 K and pore size analysis was performed by the Barret–Joyner–Halenda (BJH) method. Mercury intrusion porosimetry was performed by Micromeritics Corp.

using a Micromeritics AutoPore 9520 system. Prior to the characterization of microstructure, all samples were treated at 350 °C for 2 h in N_2 atmosphere to remove any surfactant residue.

2.4.2. Gas permeability measurement

According to the method of Smajda [14], the gas permeability of the buckypapers or carbon nanofiber paper was characterized by measuring the time dependence of the air pressure drop when exposing the buckypapers or CNF paper to a dynamic vacuum.

2.4.3. Cone calorimetry test

Combustion tests were performed on $100 \times 100 \times \sim 2.5$ mm specimens with a FTT Dual Cone Calorimeter with an exhaust flow of 24 L/s using the standardized cone calorimeter procedure (ASTM E-1354-04). Tests were performed at 50 kW/m^2 external heat flux, and three tests for each sample were conducted.

3. Results and discussion

3.1. Structures of SWCNT, MWCNT buckypapers and carbon nanofiber paper

Fig. 1 shows SEM images of the SWCNT, MWCNT buckypapers and CNF paper structures. SEM images reveal mats of fine nanotube and nanofiber, which form a random, dense, interconnected network. At high magnification views of the buckypapers and CNF paper, the SWCNT, MWCNT bundles, and individual carbon nanofiber become visible. For SWCNT and MWCNT buckypapers, CNTs have a high tendency to form bundles due to strong Van der Waals forces. For CNF paper, most of carbon nanofibers are individual due to their large diameters. Since SEM images do not contain any depth information, pore diameter readings should be regarded as apparent pore diameter measurements. The apparent pore diameters of buckypapers have a broad distribution. For SWCNT and MWCNT buckypaper, the apparent pore size distributions are between 10–50 nm and 10–100 nm, respectively. For carbon nanofiber paper, the apparent pore size is up to several hundred nanometers.

3.2. Porosity and distribution of pore sizes

Porosity and distribution of pore sizes of buckypaper and carbon nanofiber paper are important characteristics that affect gas permeability performance. Fig. 2a shows the pore size distributions from mercury intrusion porosimetry for the SWCNT, MWCNT buckypapers and the CNF paper. The pore structures are characterized by broad pore size distributions. Both MWCNT buckypaper and carbon nanofiber paper show a bimodal distribution of pore sizes. For the MWCNT buckypaper, the peak macropore size is ~200 nm and a narrow mesopore distribution is around 10 nm. For the carbon nanofiber paper, there are two pore size peaks between 100–300 nm and 300–5000 nm. The median pore sizes by volume of MWCNT buckypaper and CNF paper are 179.6 nm and 901.3 nm, respectively. The macropores arise from the macroscopic structure of the carbon nanotube or nanofiber mats, whereas the mesopores relate to the space between nanotube or nanofiber aggregates. Since resolution of micropores and mesopores by mercury porosimetry is limited by the minimum pore size in which mercury can intrude at the maximum instrument pressure, there is limitation to estimate porosity of the SWCNT buckypaper. And, due to the sheet effect, we excluded data above 5 μm [24]. The largest pore size by volume is observed in CNF paper, which has median pore diameter by volume at ~900 nm. Micropore and mesopore size distributions and BET surface area were determined by nitrogen adsorption isotherms at 77 k and pore size analysis was performed by BJH method. The pore size distributions of buckypapers and CNF paper from BJH analysis are shown in Fig. 2b. There is a wide mesopore peak at 30 nm between 10 and 80 nm in the MWCNT buckypaper pore size distribution profile. Two peaks at ~5 nm and ~10 nm are found in the SWCNT pore size distribution curve, which are related to internal pores of the nanotubes and nanotube ropes. The mesopore distribution profile of CNF paper between 10 and 100 nm is flat, which is related to small amount of aggregated carbon nanofiber. The calculated specific surface are (A_{BET}) and BJH mean pore width (d_{BJH}) are presented in Table 3. A_{BET} values of the SWCNT buckypaper (537 m^2 g^{-1}) and MWCNT (219 m^2 g^{-1}) agree well with previous report [12]. CNF paper A_{BET} value is only 24 m^2 g^{-1} because of its big diameter. Since in BJH method only pores in size between 0.1 and 100 nm were calculated, however, most of pores in CNF paper are distributed between 100 and 5000 nm based on the mercury porosimetry. Therefore, the average pore size in CNF paper (19.6 nm) determined by BJH method (4V/A) is underestimated. In summary, SWCNT and MWCNT buckypapers show much smaller pore sizes than CNF paper, which means both of them have a compact carbon nanotube network.

3.3. Gas permeability

Since the proposed flame retardant mechanism of buckypapers or CNF paper is that preformed carbon nanotubes or a nanofiber sheet acts as a shield to reduce or delay the combustible gases release from polymer underneath and separate them from the oxygen to prevent the combustion process being sustained, the resistance to gas flow is the key performance of the buckypapers and CNF paper as shields. The gas permeability (or resistance to airflow) of buckypaper and CNF paper was characterized by measuring the pressure decay in a gas reservoir which could only lose gas through the buckypapers or CNF paper. Pressure (p) in the reservoir as a function of time, t, could be described by a first order exponential decay as given in Eq. (1):

$$p(t) = const + p_0 e^{-\frac{t}{\tau}} \quad (1)$$

where p_0 [Pa] is the pressure in the reservoir at the start of the evaluation and the time constant τ can be expressed as:

$$\tau = \frac{V_u \times l}{A \times R \times T \times D_{eff}} \quad (2)$$

In Eq. (2), V_u [m^3] is the volume of the reservoir, l [m] is the thickness of buckypapers or CNF paper, A [m^2] is the surface of buckypapers or CNF paper, R [J mol^{-1} K^{-1}] is the universal

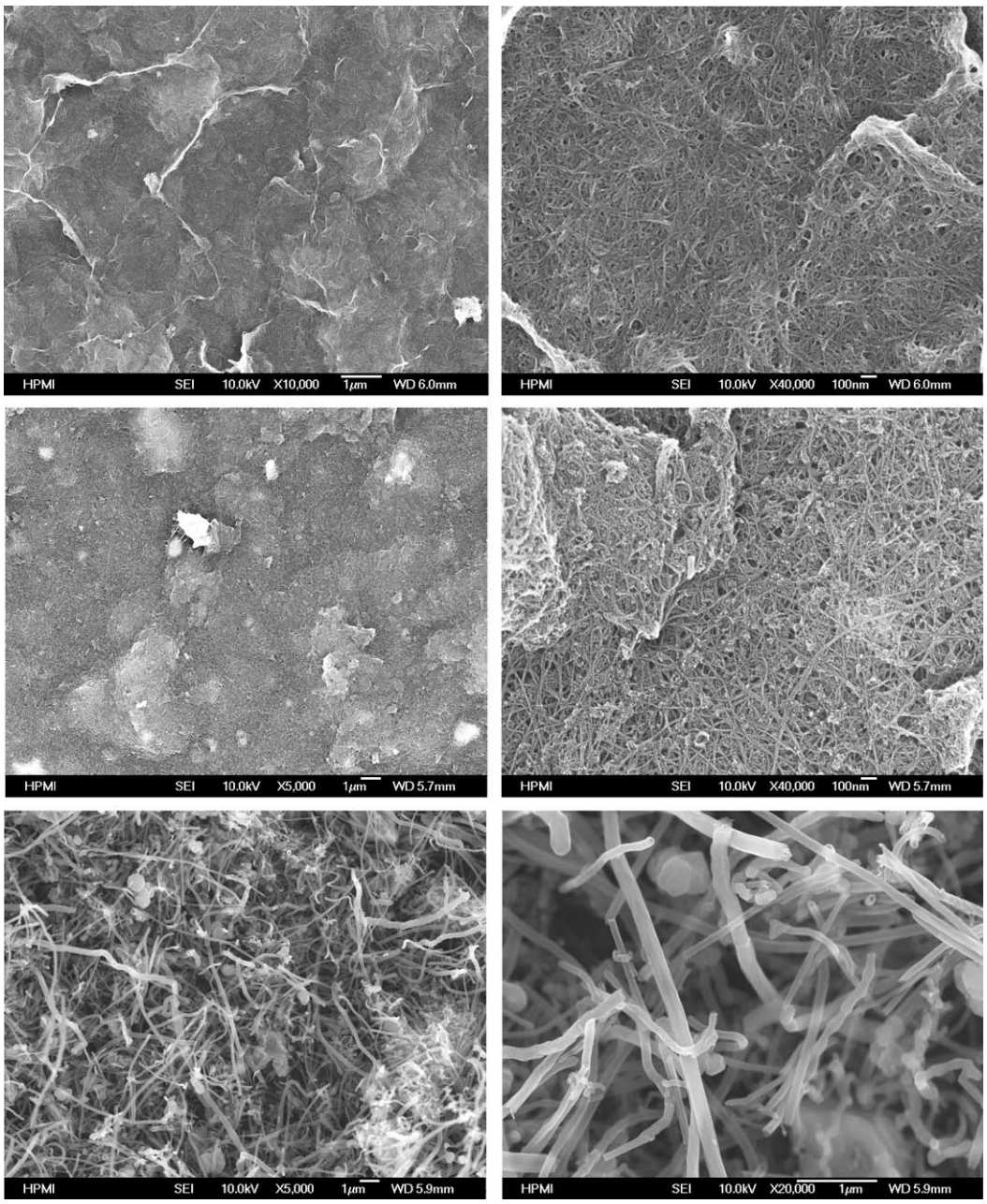

Fig. 1 – SEM images of SWCNT, MWCNT buckypaper and CNF paper (from top to bottom). Left: low magnification; right: high magnification.

gas constant and T [K] is the temperature. Fig. 3 presents pressure drop curves measured with air through buckypapers and CNF paper. The effective diffusivity D_{eff} [mol Pa^{-1} m^{-1} s^{-1}] was calculated from Eq. (2) according to pressure drop curves shown in Fig. 5. In general, gas flow decreases with increasing filter thickness and density of nanotube or nanofiber, and is proportional to the diameter of nanotube or nanofiber in the buckypapers or CNF paper. The differences in pressure drop can be directly attributed to differences in the nanotube or nanofiber network. In Fig. 4 it can be found that pressure drop of CNF paper is the fastest due to its largest pore size and porosity although it is the thickest membrane used in the current study. By comparing SWCNT and MWCNT buckypaper pressure drop curves, MWNCT buckypaper shows slower pressure drop than that of SWCNT buckypaper, although SWCNT buckypaper has the lowest air effective diffusivities (Table 4), which can be attributed to the thickness advantage of MWCNT buckypaper.

3.4. *Cone calorimeter test*

The cone calorimetry has been widely used to evaluate the flammability characteristics of materials because its results correlate well with those obtained from large-scale fire tests and can be used to predict the combustion behavior of materials in real fires [25,26]. The principle of cone calorimeter experiments is based on the oxygen consumption that the gross heat of combustion of any organic material is directly

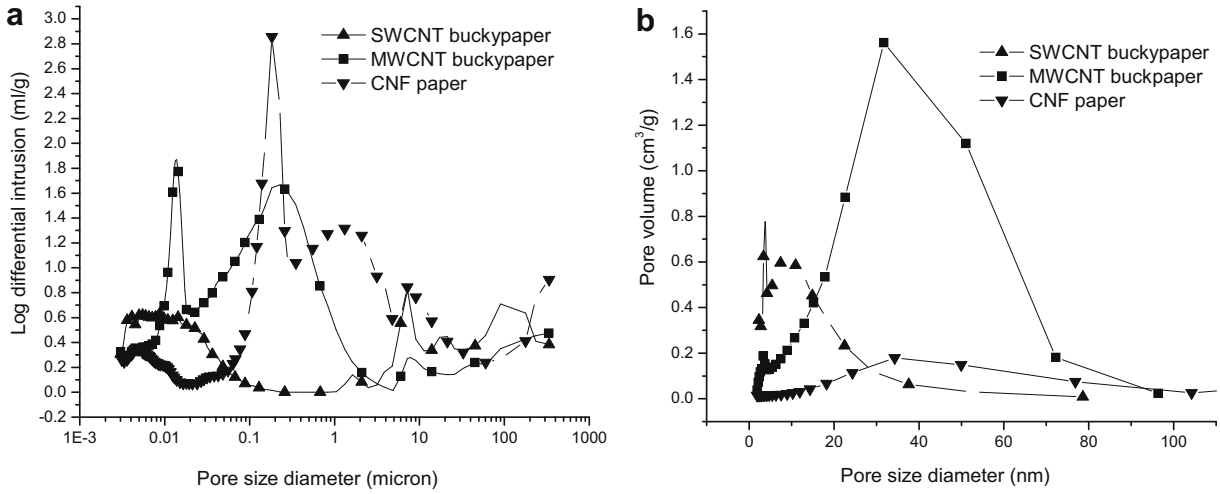

Fig. 2 – Pore structures of SWCNT, MWCNT buckypaper and CNF paper. (a) Pore size distributions from mercury intrusion porosimetry. (b) BJH pore analysis of the buckypapers and CNF paper.

Table 3 – Porosity of buckypapers and CNF paper derived from mercury porosimetry and N_2 adsorption measurements.

Sample	N_2 isotherms	Adsorption	Mercury intrusion porosimetry		
	A_{BET} ($m^2\ g^{-1}$)	d_{BJH} (nm)	Average pore diameter (4V/A) (nm)	Median pore diameter (volume) (nm)	Porosity (%)
SWCNT buckypaper	537	4.8	22.6	10	76.6
MWCNT buckypaper	174.3	14.9	37.8	179.6	85.9
CNF paper	24	19.6	85.0	901.3	90.8

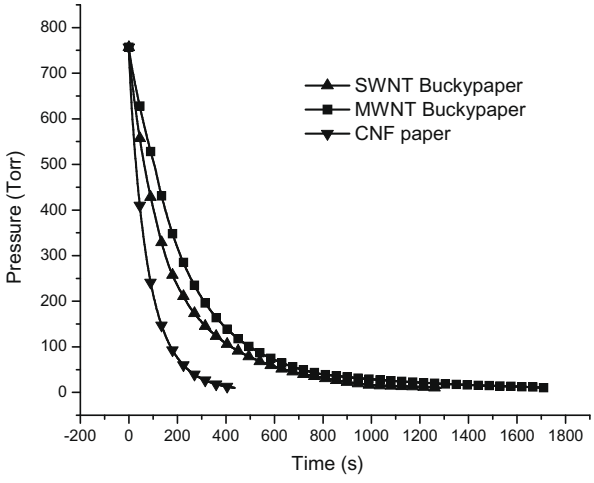

Fig. 3 – Pressure drop curves of gas flow through SWCNT buckypaper, MWCNT buckypaper and CNF paper.

related to the amount of oxygen required for combustion. Most organic materials release a quantity of heat practically proportional to the quantity of oxygen consumed while burning. Approximately 13.1 MJ of heat are released per kilogram of oxygen consumed [27]. The measurement of the decreasing oxygen concentration in the combustion gases of a sample subjected to a given heat flux (in general from 10 to 100 kW/m^2) is used to calculate the quantity of heat released per unit of time and surface area. The heat release rate (HRR) over time, in particular the value of its peak (peak of HRR), is usually taken into account in order to evaluate the fire behavior. In addition, the cone calorimeter test also determined a number of properties simultaneously. Table 5 reports the main parameters for each material obtained from cone calorimeter measurements. The parameters, which will be addressed, include time to ignition (TTI), heat release rate (HRR), total heat released (THR), total smoke released (TSR), maximum average rate of heat emission (MAHRE), and total mass loss during combustion.

TTIs for composites Epoxy/IM-7/buckypaper or CNF paper appear delayed with respect to Epoxy/IM-7 composite, and a remarkable delay is observed for Epoxy/IM-7/MWCNT buckypaper. Polymer combustion starts with polymer bond scission due to an increase in the temperature. The volatile fraction of the resulting polymer fragments diffuses into the air and creates a combustible gaseous mixture. This gaseous mixture ignites when its concentration reaches the critical point and the auto-ignition temperature is reached. Although buckypapers and carbon nanofiber paper have higher thermal conductivity, which conducts higher temperature on the composites' surface, the presence of buckypapers or CNF paper can act as barrier to reduce the release of polymer fragments from matrix underneath into the air, which delays time to the critical point of the concentration of combustible gases. Based on TTI from cone calorimetry test, the shield

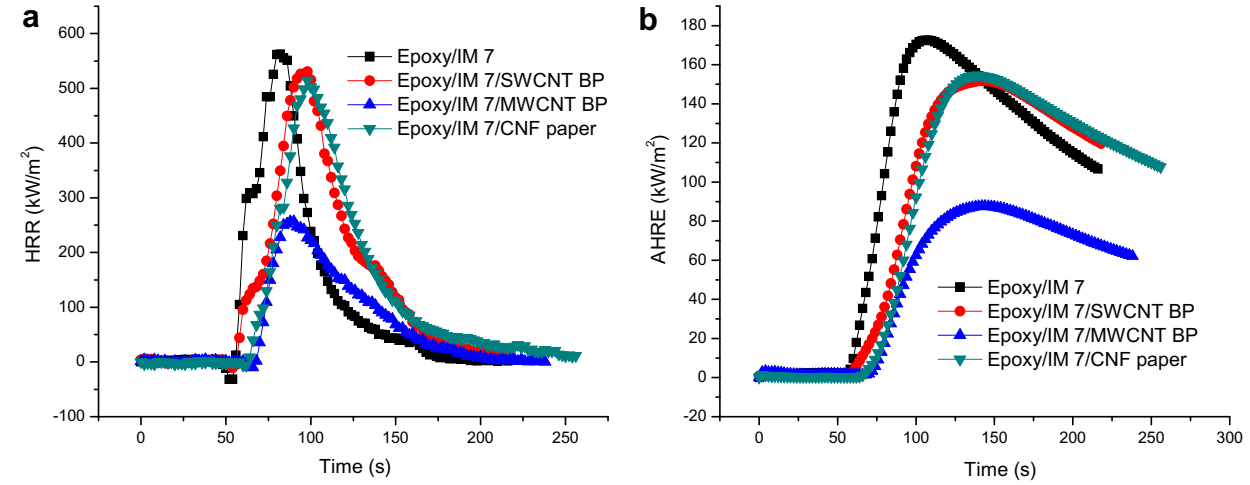

Fig. 4 – Comparison of heat release rate curves and average rate (a) of heat emission curves (b) for Epoxy/IM-7, Epoxy/IM-7/SWCNT-BP, Epoxy/IM-7/MWCNT-BP and Epoxy/IM-7/CNF paper.

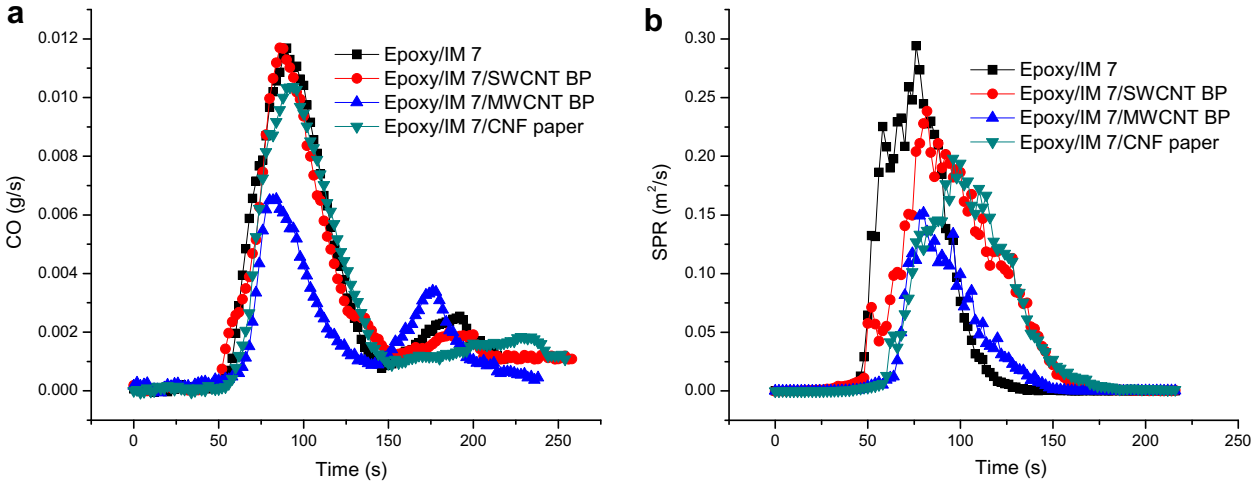

Fig. 5 – Comparison of CO production rate (a) and smoke production rate (b) during combustion.

Table 4 – Effective diffusivities of air in the current buckypaper and CNF paper.

Sample	SWCNT buckypaper	MWCNT buckypaper	CNF paper
D_{eff} (10^{-9} mol Pa^{-1} m^{-1} s^{-1})	1.87	3.63	18.6

effect of buckypapers or carbon nanofiber paper is predominated. Less resin inside the top buckypaper or CNF paper layers due to their carbon rich area might also be responsible for the delayed ignition time.

Fig. 4a shows a comparison of heat release rate curves for Epoxy/IM-7, Epoxy/IM-7/SWCNT-BP, Epoxy/IM-7/MWCNT-BP and Epoxy/IM-7/CNF paper. The heat release rate curves of the Epoxy/IM-7/SWCNT-BP and Epoxy/IM-7/CNF paper composites show the similar trend as that of the Epoxy/IM-7 composite, whereas a remarkable reduction was observed for Epoxy/IM-7/MWCNT-BP. The peak heat release rate of the Epoxy/IM-7/MWCNT-BP composite is about 45% of that of the Epoxy/IM-7 composite. Heat release curves also show the delay of the Time-to-Peak HRR for Epoxy/IM-7/BP or CNF paper composites compared to Epoxy/IM-7 composites. THR in Table 5 is the integral of heat release rate curves over the duration of the experiment The value of THR in Table 5, of the Epoxy/IM-7/MWCNT-BP composite is 60% of that of the Epoxy/IM-7 composite, whereas THR value of the Epoxy/IM-7/SWCNT-BP and Epoxy/IM-7/CNF paper are close to that of the Epoxy/IM-7 composite. The reduction of THR values indicates that the presence of buckypaper can restrict fire development or even extinguish a fire. A reduction in mass loss during the combustion can be found in the Epoxy/IM-7/MWCNT-BP composites. The values of total mass loss are reported in Table 5. The mass loss is mainly from the epoxy decomposition. The total mass loss of Epoxy/IM-7, Epoxy/IM-7/SWCNT-BP and Epoxy/IM-7/CNF paper is around 80 wt.% of epoxy in the original composites, whereas in the case of Epoxy/IM-7/MWCNT-BP composites, only 50% mass of

Table 5 – Main parameters from cone calorimeter measurements.

Sample	TTI (s)	Peak HRR (kW/m^2)	Time to peak HRR (s)	THR (MJ/m^2)	TSR (m^2/m^2)	MAHRE	Total mass loss (g)	Sample weight (g)
Epoxy/IM-7	46 ± 2	568 ± 6	84 ± 2	23.2 ± 1.1	1123.7 ± 53	179 ± 4	10.6 ± 0.2	36.6 ± 0.3
Epoxy/IM-7/SWCNT-BP	50 ± 4	526 ± 7	95 ± 3	24.5 ± 1.3	1180.1 ± 42	152 ± 4	10.8 ± 0.2	37.4 ± 0.4
Epoxy/IM-7/MWCNT-BP	64 ± 4	258 ± 5	90 ± 3	13.2 ± 0.9	526.1 ± 26	82 ± 6	6.2 ± 0.1	37.2 ± 0.3
Epoxy/IM-7/CNF paper	59 ± 3	508 ± 5	96 ± 3	24.8 ± 1.3	1165.3 ± 37	158 ± 6	10.8 ± 0.2	38.0 ± 0.4

epoxy was lost during the test. The presence of MWCNT buckypaper accumulated the polyaromatic hydrocarbons and prevented them from pyrolysis and subsequent oxidation/combustion. MWCNT buckypaper reduces the mass loss during the combustion, which is directly relative to the THR values.

Fig. 4b shows the average rate of heat emission (AHRE) curves. This parameter is defined as the cumulative heat emission divided by time and its peak value (maximum average rate of heat emission, MAHRE) and has been proposed as a good measure of the propensity for fire development under real scale condition. MAHRE for Epoxy/IM-7/MWCNT BP in Table 5 shows a dramatic reduction (~50%) with respect to control sample, whereas Epoxy/IM-7/SWCNT-BP and Epoxy/IM-7/CNF paper composites only have ~15% reduction.

Smoke and toxic gases generated during combustion are the other two important factors concerning fire safety: heavy smoke can hinder escape and toxic gases act as the killer during the fire hazard. Fig. 5a and Table 5 report smoke production parameters. The values of the smoke production rate (SPR) and total smoke released (TSR) of the Epoxy/IM-7/MWCNT buckypaper composite were reduced by more than 50% compared to the Epoxy/IM-7 composite. The smoke production is ascribed to the thermal decomposition of resins, which leads to aromatic volatiles in the flame, resulting in a soot increase. The peak of the smoke production rate of the composite with CNF paper shows a delay, which means that the CNF paper can act as a physical barrier to limit soot transfer. Fig. 5b shows the CO production significantly decreased in CO yield due to the MWCNT buckypaper skin, which also can be attributed to the reduction of mass loss. The less mass lost during fire test, the less heat released, the less smoke and CO generated.

The different flame retardant efficiencies of SWCNT, MWCNT buckypapers and CNF paper can be attributed to their specific properties. The median pore diameter of CNF paper determined by mercury intrusion porosimetry is around 900 nm, which is responsible for its high gas permeability. The presence of CNF paper on the composite surface cannot resist decomposed gas release efficiently. In the case of composite with SWCNT buckypaper, it can be found the SWCNT buckypaper was burnt away after combustion and there is only red iron catalyst residue left on the fiber surface after the cone calorimetry test. The thermal stability of SWCNT is not good enough to survive during this fire test, therefore SWCNT buckypaper cannot act as fire shield to protect the Epoxy/IM-7 composite underneath. But in the previous research [20], SWCNT buckypaper showed good flame retardancy on the surface of a POSS/glass fiber composite. The main reason is that the residue from POSS is thermally stable ceramic char, which shields the underlying SWCNT paper from the radiated heat and limits SWCNT oxidation, thus SWCNT maintaining its dense network and protecting the polymer underneath. The different fire performance of SWCNT buckypaper in Epoxy/IM-7 and bismaleimide (BMI)/IM 7 composites has been discussed somewhere else [28]. Briefly, due to the synergistic effect between SWCNT buckypaper and BMI (or residues of BMI), the buckypaper can survive and keep its dense structure during fire test, thus acting as a fire-blocking layer protecting underlying polymer composites, while SWCNT buckypaper on Epoxy/IM-7 composites was consumed by oxidation at high temperature during fire test. By combining high thermal stability and gas resistance to gas flow, MWCNT buckypaper reduced the fire hazard of Epoxy/IM-7 composite by acting as a fire shield, which makes it a promising novel material to improve flame retardancy of polymeric composites.

4. Conclusions

SWCNT, MWCNT buckypaper and CNF paper as proposed fire shields were applied to the surface of epoxy carbon fiber composites. Their flammability behaviors were investigated by cone calorimeter. The thermo-oxidation stability and low gas permeability of buckypapers or CNF nanofiber are key roles in improving flame retardant properties of composites. In the cone calorimeter test condition, the MWCNT-based buckypaper, due to its high temperature thermo-oxidation and dense network, acted as an effective fire shield to reduce heat, smoke, and toxic gases generated during fire combustion. SWCNT-based buckypaper was burnt out after combustion in the Epoxy/IM-7/SWCNT-BP composite and did not affect the flammability of the composite. In the case of Epoxy/IM-7/CNF paper composite, the big pore size of the CNF paper network resulted in high gas permeability, which was the reason for its low flame retardant efficiency.

REFERENCES

[1] Baughman RH, Zakhidov AA, de Heer WA. Carbon nanotubes-the route toward applications. Science 2002;297:787–92.
[2] Wong EW, Sheehan PE, Lieber CM. Nanobeam mechanics: elasticity, strength, and toughness of nanorodes and nanotubes. Science 1997;277:1971–5.
[3] Tans SJ, Verschueren ARM, Dekker C. Room temperature transistor based on a single carbon nanotube. Nature 1998;393:49–51.
[4] Kong J, Franklin NR, Zhou C, Chapline MG, Peng S, Cho K, et al. Nanotube molecular wires as chemical sensors. Science 2000;287:622–5.

[5] Ajayan PM, Schadler LS, Giannaries C, Rubio A. Single-walled carbon nanotube-polymer composites: strength and weakness. Adv Mater 2000;12:750–3.
[6] Kashiwagi T, Du F, Winey KI, Groth KM, Shields JR, Bellayer SP, et al. Thermal and flammability properties of polypropylene/carbon nanotube nanocomposites. Polymer 2005;46:471–81.
[7] Kashiwagi T, Du F, Douglas JF, Winey KI, Harris RH, Shields JR. Nanoparticle networks reduced the flammability of polymer nanocomposites. Nat Mater 2005;4:928–33.
[8] Cipiriano BH, Kashiwagi T, Raghavan SR, Yang Y, Grulke EA, Yamamoto K, et al. Effects of aspect ratio of MWNT on the flammability properties of polymer nanocomposites. Polymer 2007;48:6086–96.
[9] Kashiwagi T, Mu M, Winey K, Cipriano B, Raghavan SR, Pack S, et al. Relation between the viscoelastic and flammability properties of polymer nanocomposites. Polymer 2008;49:4358–68.
[10] Liu J, Rinzler AG, Dai HJ, Hafner JH, Bradley RK, Boul PJ, et al. Fullerene pipes. Science 1998;280:1253–6.
[11] Bae DJ. Transport phenomena in an anisotropically aligned single-wall carbon nanotube film. Phys Rev B 2001:64 [Art. no. 233401-4].
[12] Knapp W, Schleussner D. Field-emission characteristics of carbon buckypaper. J Vac Sci Technol B 2003;2:557–68.
[13] Cooper SM. Gas permeability of a buckypaper membrane. Nano Lett 2003;3:189–92.
[14] Smajda R, Kukovecz A′, Ko′nya Z, Kiricsi I. Structure and gas permeability of multi-wall carbon nanotube buckypapers. Carbon 2007;45(6):1176–84.
[15] Viswanathan G, Kane DB, Lipowicz PJ. High efficiency fine particulate filtration using carbon nanotube coatings. Adv Mater 2004;16:2045–9.
[16] Zhang XF, Sreekumar TV, Liu T, Kumar S. Properties and structure of nitric acid oxidized single wall carbon nanotube films. J Phys Chem B 2004;108:16435–40.
[17] Baughman RH, Cui CX, Zakhidov AA, Iqbal Z, Barisci JN, Spinks GM, et al. Carbon nanotube actuators. Science 1999;284:1340–4.
[18] Vohrer U, Kolaric I, Haque MH, Roth S, Weglikowska UD. Carbon nanotube sheets for the use as artificial muscles. Carbon 2004;42:1159–64.
[19] Dharap P, Li ZL, Nagarajaiah S, Barrera EV. Nanotube film based on single-wall carbon nanotubes for strain sensing. Nanotechnology 2004;15:379–82.
[20] Chen YW, Miao HY, Zhang M, et al. Analysis of a laser post-process on a buckypaper field emitter for high and uniform electron emission. Nanotechnology 2009;20:325302.
[21] Wang Z, Liang Z, Wang B, Zhang C, Kramer L. Processing and property investigation of single-walled carbon nanotube (SWNT) buckypaper/epoxy resin matrix nanocomposites. Compos Part A: Appl Sci Manuf 2004;5:1225–32.
[22] Wu Q, Zhang C, Liang ZY, Wang B. Fire retardancy of a buckypaper membrane. Carbon 2008;46:1164–5.
[23] Zhao ZF, Gou JH, Bietto S, Ibeh C, Hui D. Fire retardancy of clay/carbon nanofiber hybrid sheet in fiber reinforced polymer composites. Compos Sci Technol 2009;69:2081–7.
[24] Whitby RLD, Fukuda T, Maekawa T, James SL, Mikhalovsky SV. Geometric control and tuneable pore size distribution of buckypaper and buckydiscs. Carbon 2008;46:949–56.
[25] Schartel B, Bartholmai M, Knoll U. Some comments on the use of cone calorimter data. Polym Degrad Stab 2005;88:540–7.
[26] Laoutid F, Bonnaud L, Alexandre M, Lopez-Cuesta JM, Dubois Ph. New prospects in flame retardant polymer materials: from fundamental to nanocomposites. Mater Sci Eng 2009;63:100–25.
[27] Huggett C. Estimation of rate of heat release by means of oxygen consumption measurements. Fire Mater 1980;4:61–5.
[28] Wu Q, Bao JW, Zhang C, Liang ZY, Wang B. Enhancement of flame retardancy in epoxy and bismaleimide/carbon fiber composites by the incorporation of buckypaper on the composite surface. SAMPE Fall Tech Conf, Memphis, 2008.